High dynamic range interferometric observations of exozodiacal discs: performance comparison between ground, space and Antarctica

Olivier Absil[a], Denis Defrère[b], Vincent Coudé du Foresto[c], Emmanuel Di Folco[d], Roland den Hartog[e], Jean-Charles Augereau[a]

[a]LAOG–UMR 5571, CNRS and Université Joseph Fourier, BP 53, F-38041 Grenoble, France;
[b]Institut d'Astrophysique et de Géophysique, Université de Liège, 17 Allée du Six Août, B-4000 Liège, Belgium;
[c]LESIA–UMR 8109, CNRS and Observatoire de Paris-Meudon, 5 place J. Janssen, F-92195 Meudon, France;
[d]Observatoire Astronomique de l'Université de Genève, 51 chemin des Maillettes, CH-1290 Sauverny, Switzerland;
[e]Science Payloads and Advanced Concepts Office, ESA/ESTEC, postbus 299, NL-2200 AG Noordwijk, The Netherlands.

ABSTRACT

The possible presence of large amounts of exozodiacal dust around nearby main sequence stars represents a threat to the detection and characterisation of Earth-like extrasolar planets with future infrared space interferometers such as Darwin or TPF. In this paper, we first review the current detection capabilities of ground-based infrared interferometers such as CHARA/FLUOR and the detections of hot dust that have been obtained so far around a few main sequence stars. With the help of realistic instrumental simulations, we then discuss the relative merits of various ground-based sites (temperate and Antarctic) versus space-based observatories for the detection of exozodiacal discs down to a few zodi by interferometric nulling as a preparation to future life-finding missions. In particular, we discuss the performance of four proposed nulling interferometers: GENIE, ALADDIN, Pegase and FKSI. An optimised strategy for the characterisation of candidate Darwin/TPF targets is finally proposed.

Keywords: Exozodiacal dust, infrared interferometry, nulling interferometry, high-dynamic range observations

1. INTRODUCTION

Debris discs are optically-thin, gas-poor dust discs around main-sequence (MS) stars. The presence of circumstellar dust around stars with ages above ~ 10 Myr is attributed to populations of planetesimals that were neither used to make up planets nor ejected from the system by the time when the nebular gas is dispersed. These leftovers produce dust by mutual collisions and comet-type activity. Being continuously replenished by small bodies, the disc can then persist over much of the star's lifetime. Due to its large total cross-section area, dust is much easier to observe than planets, not speaking of planetesimals. On the other hand, distributions of dust respond to the presence of planetary perturbers, reflect distributions of the parent bodies and bear important "memory" of the planetary formation process in the past. Hence debris discs can be used as sensitive tracers of directly invisible planets, as well as small body populations, and should reflect evolutionary stages of planetary systems. This explains substantial effort invested into observations and theoretical modelling of debris discs in the last decade.

In the case of our solar system, the planetary region is immersed in a tenuous sheet of dust, called zodiacal cloud. Its properties have been subject to intensive studies over decades.[1] Even though the zodiacal cloud is the most luminous component of the solar system after the Sun, it is thought to be a relatively dust-poor inner part in the actual debris disc which encompasses the Edgeworth-Kuiper belt (EKB) region. The extensions, mass,

Send correspondence to O.A. (olivier.absil@obs.ujf-grenoble.fr)

and cross-section area of the latter should by far supersede those of the zodiacal cloud. Ironically, this disc has not been observed yet, due to its extremely low optical depth and to the fact that remote sensing "from inside" is naturally more difficult. Nevertheless, there are some indications for its existence in spacecraft in-situ data.[2]

The situation with other stars is completely reverse. Cold dust emission has been found for hundreds of stars, strongly suggesting the existence of extrasolar Kuiper belts. Mid- to far-infrared space observatories (e.g., SPITZER) are revolutionising the field, allowing analysis of outer discs at a statistical level. However, information on exozodiacal clouds, i.e., on dust in the inner, planetary region of the extrasolar systems is extremely scarce. As recognised by the European and American Space Agencies, exozodiacal dust in the habitable zone around nearby stars is actually a significant source of background flux that must be considered in any effort to image terrestrial planets*. While our current knowledge of exozodiacal dust clouds is almost exclusively based on the Solar System, the amount of warm dust that can be expected around nearby main sequence stars is actually one of the main design drivers for the DARWIN/TPF missions. In practice, it is estimated that the detection and characterisation of habitable terrestrial planets would be seriously hampered for stars presenting warm ($\sim 300\,\mathrm{K}$) exozodiacal dust more than ~ 20 times as dense as our solar zodiacal cloud.[3]

In this paper, we review the ground-based interferometric efforts towards the characterisation of DARWIN/TPF target stars through the characterisation of the warm dust density level in their habitable zone. The first detections that have been obtained with classical $\mathcal{V}^2$ interferometers are first discussed. Then, we simulate the performance of proposed ground- and space-based nulling interferometry precursors to the DARWIN/TPF mission such as GENIE, ALADDIN, PEGASE, or the FKSI. We have limited our comparison to instruments working at similar wavelengths (ranging from 2 to $8\,\mu$m), and purposely discarded ground-based instruments working in the N-band such as the Keck Interferometer Nuller and the LBTI. The ultimate performance of these two mid-infrared instruments essentially depends on the spatial and temporal fluctuations of the sky and instrumental thermal backgrounds, which are very difficult to model with a sufficient accuracy for our modelling purpose. Our simulations take into account the turbulence characteristics and vibrational environment of the various sites, as well as the preliminary design of these instruments. Based on these simulations and on the current performance of ground-based (nulling) interferometers, we propose an optimised strategy for the detection of exozodiacal discs around DARWIN/TPF candidate targets. In particular, the relative merits of the various sites are discussed.

2. CURRENT PERFORMANCE OF GROUND-BASED INSTRUMENTS

Although simple photometric measurements are in principle capable of detecting warm dust in exozodiacal clouds, the performance of even the best space-based infrared spectro-photometric instruments (e.g., IRAC and IRS on SPITZER) have been limited to fractional luminosities L_{dust}/L_* as high as 1400 times the solar zodiacal cloud in the 8–13 μm regime.[4] This is due to the high luminosity of stellar photospheres in the near- to mid-infrared regime, which generally hides the signature of warm dust grains. Resolving the star-disc system with high angular resolution observations is a natural way to mitigate this limitation, and pioneering observations of inner debris discs have been obtained in the last few years with high-precision near-infrared interferometers. In this section, we review the detections that have been published so far, and discuss the limiting sensitivity of such instruments.

2.1 Principle of debris disc detection

The principle of debris disc detection by classical "$\mathcal{V}^2$" stellar interferometry is based on the fact that the stellar photosphere and its surrounding dust disc have different spatial scales. For an A-type star at a distance of 20 pc, the angular diameter of the photosphere is typically about 1 mas, while the circumstellar disc extends beyond the sublimation radius of dust grains, typically located around 10 to 20 mas for black body grains sublimating at $T_{\mathrm{sub}} \simeq 1500\,\mathrm{K}$. In the infrared K band, the debris disc is therefore generally fully resolved at short baselines ($10 - 20\,\mathrm{m}$), while the photosphere is only resolved at long baselines ($\sim$200 m). One can take advantage of this fact to isolate the contribution of circumstellar dust by performing visibility measurements at short baselines, where the stellar photosphere is almost unresolved. The presence of resolved circumstellar emission then shows

*See e.g. the NASA Exoplanet Task Force Report at http://www.nsf.gov/mps/ast/exoptf.jsp.

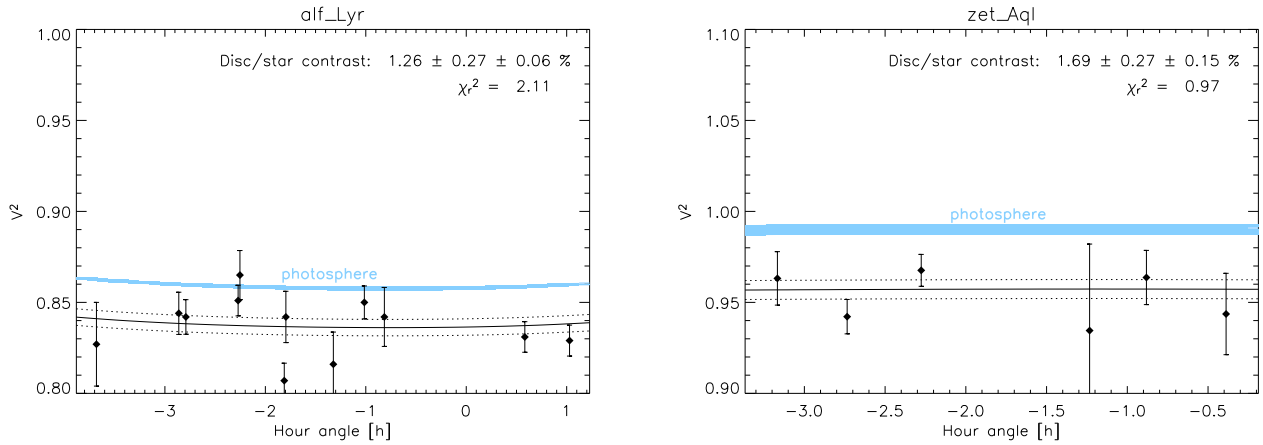

Figure 1. Detection of circumstellar emission around two A-type stars with CHARA/FLUOR (*left*: Vega, *right*: ζ Aql).[10,11] The squared visibilities are plotted with their error bars as a function of hour angle on the CHARA S1–S2 baseline (33 m). The blue region represents the 1σ box defined by our semi-empirical photospheric models. We have fitted to our data a model of a limb-darkened photosphere surrounded by a uniform circumstellar emission. The best-fit model is represented by the black solid line, while the dotted lines represent the 1σ statistical uncertainty on the best-fit model. Circumstellar emission is detected when the blue region lies significantly above the uppermost dotted line. The inferred contrast between the uniform circumstellar emission and the star is given as inset for each star ("disc/star contrast"), together with its two error bars (the first one is related to the statistical dispersion of the calibrated data set and the second one to the uncertainty on the photospheric model) as well as the reduced χ^2 of the fit.

up as a deficit of squared visibility with respect to the expected visibility of the bare stellar photosphere, as shown in:[5]

$$\mathcal{V}^2(B) \simeq (1 - 2\epsilon_{\rm CSE})\mathcal{V}_*^2(B)\,, \tag{1}$$

where $\mathcal{V}^2$ and $\mathcal{V}_*^2$ are respectively the squared visibility of the star-disc system and of the bare stellar photosphere, B the interferometer baseline length, and $\epsilon_{\rm CSE}$ the flux ratio between the integrated circumstellar emission within the field-of-view and the stellar photospheric emission. This equation is valid only for short baselines and for $\epsilon_{\rm CSE} \ll 1$, as expected for an optically and geometrically thin circumstellar disc.

Due to the expected faintness of the circumstellar emission ($\epsilon_{\rm CSE} \leq 1\%$), detection needs both a high accuracy on the measured $\mathcal{V}^2$ and on the estimation of the squared visibility $\mathcal{V}_*^2$ of the bare photosphere at short baselines. While the former has already been demonstrated in the framework of single-mode near-infrared interferometers,[6] the latter is ensured to a large extent by the fact that the stellar photosphere is almost unresolved at short baselines, so that we can tolerate a certain level of imprecision on the knowledge of the stellar angular diameter without jeopardising the detection. For instance, a stellar photosphere with an angular diameter of 1.0 ± 0.1 mas produces a squared visibility of 0.995 ± 0.001 at a baseline of 20 m in the K band. Limb-darkening is a negligible effect as well at such baselines. Therefore, diameter measurements at long interferometric baselines are not mandatory to derive accurate photospheric models, and empirical surface-brightness relations[7] can instead be used to predict stellar angular diameters with a sufficient accuracy, taking into account rotational distortion with a simple hydrostatic equilibrium model based on the measured $v \sin i$ of the star.

2.2 Recent observational results

Two interferometric instruments have already provided useful constraints on exozodiacal emission around nearby main sequence stars: FLUOR at the CHARA Array and VINCI at the VLTI. We will not discuss here the recent observations obtained with the Keck Nulling Interferometer (KIN), which are the subject of another paper at this conference[8] and have not been published yet.

Figures 1 and 2 give an overview of the observational results that have been obtained so far respectively on A-type and Sun-like stars. As a first step, observations with VLTI/VINCI[9] provided meaningful upper limits

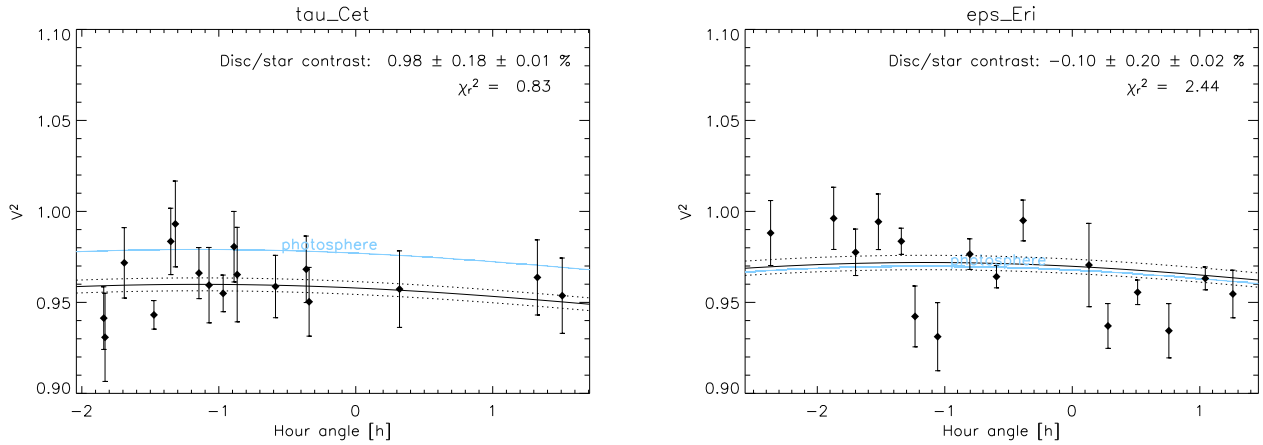

Figure 2. Two observational results on Sun-like stars with CHARA/FLUOR (*left*: detection around τ Cet, *right*: non-detection around ϵ Eri).[5] Same conventions as in Fig. 1.

of a few percent on the disc/star contrast for five stars of various types. The first secure detection was then obtained with CHARA/FLUOR around Vega.[10] Based on this success, a survey of nearby debris disc stars was then initiated, leading to new detections around τ Cet[5] and ζ Aql,[11] as well as a possible detection around β Leo (Akeson et al., submitted). Non-detections have also been reported around five A-type stars[11] and around ϵ Eri.[5]

Although the presence of hot dust is not the unique solution to explain the observed visibility deficit for some of these stars, these results provide direct estimations of the sensitivity of current near-infrared single-mode interferometers to exozodiacal dust discs. In particular, we note that a typical 1σ error bar of 0.2% on the disc/star contrast can be reached in the K band for one full night of observation (corresponding to about 15 single measurements with the FLUOR instrument). This K-band flux ratio can be compared to the case of the solar zodiacal cloud, even though further modelling of inner debris discs detected by infrared interferometry has shown that the dust density and size distributions are very different from that of our local zodiacal cloud. A K-band flux ratio of 0.2% theoretically corresponds to an exozodiacal dust cloud about 1000 times as dense as the solar zodiacal cloud, based on the K-band flux ratio between the solar zodiacal cloud (Kelsall model[13]) and the Sun. Thus, near-infrared interferometry currently achieves performance similar to Spitzer for the detection of exozodiacal clouds. However, it must be noted that, because near-infrared interferometry is sensitive to dust at much higher temperature (close to the sublimation limit), the dust mass that has been inferred around Vega, τ Cet and ζ Aql is only about 10^{-9} to $10^{-7}\,M_\oplus$, which is in fact equivalent to the mass of the local zodiacal cloud! This further indicates that dedicated modelling efforts (beyond the simple solar-like zodiacal cloud model) are necessary to interpret the resolved observations of exozodiacal discs.

3. PERFORMANCE SIMULATION IN NULLING INTERFEROMETRY

The performance of current "classical" interferometric facilities for the detection of faint exozodiacal discs is obviously limited by the large flux ratio between the star and its surrounding dust cloud. In order to improve the situation, nulling interferometry can be used to reduce the stellar flux by destructive interference while letting through a large part of the circumstellar emission. A two-telescope nulling interferometer is characterised by its transmission map $T_\lambda(\theta,\phi)$, which takes the following form assuming that the field-of-view is diffraction limited and that a pure π phase shift has been applied to one arm of the interferometer:

$$T_\lambda(\theta,\phi) = \left(\frac{2J_1(\pi\theta D/\lambda)}{\pi\theta D/\lambda}\right)^2 \sin^2\left(\pi\frac{B\theta}{\lambda}\cos\phi\right) , \qquad (2)$$

where θ and ϕ are respectively the radial and polar angular coordinates with respect to the optical axis, B the interferometer baseline, D the telescope diameter and λ the wavelength. In the following study, we assume that

recombination and detection are both done in the pupil plane, so that no image is formed: the flux coming from the various sources in the field-of-view is first affected by the local value of the transmission map, then integrated across the whole field-of-view and finally detected on a single pixel. Performing the detection in an image plane would not significantly change the conclusions of this study.

In order to evaluate the performance of future nulling interferometry instruments, we have developed a software simulator, called *GENIEsim*, which performs end-to-end simulations of nulling interferometers using a system-based architecture. In this section, we briefly describe the main building blocks and physical processes included in GENIEsim. The interested reader can find more information on the simulator in a previous paper.[12]

3.1 Signals and noises in nulling interferometry

A variety of astrophysical and non-astrophysical sources contribute to the final signal at the destructive output of a nulling interferometer. This section gives a brief overview of each of them, assuming that planets do not contribute significantly to the overall photon budget (main-sequence stars surrounded by hot giant planets are not discussed in this study).

- *Exozodiacal dust disc*—In this study, we will assume that exozodiacal dust discs follow the same density distribution as in the solar system, using the model of Kelsall.[13] Only a global density scaling factor will be applied—we will use the denomination "**zodi**" for this parameter. As discussed in the introduction, the goal of future nulling instruments should be to reach exozodiacal dust densities as low as 20 zodis.

- *Stellar leakage*—Part of the incoming stellar photons make it to the destructive output of the nulling interferometer due to two effects: the finite size of the stellar photosphere, and the combined effect of atmospheric and instrumental errors. The first phenomenon, known as geometric stellar leakage, is deterministic and the associated nulling ratio N can be evaluated through the following equation:

$$N = \frac{\pi^2}{4} \left(\frac{B\theta_*}{\lambda} \right)^2 , \tag{3}$$

  assuming a uniform brightness across the stellar disc. The second phenomenon is caused by the imperfect cophasing of the beams, intensity mismatches and polarisation errors, which can be due either to atmospheric turbulence or to instrumental imperfections (including vibrations). It adds to the geometric leakage at the destructive output of the interferometer. Instrumental leakage has two effects on the performance of the nuller: first, it introduces a *bias*, the mean contribution of instrumental leakage, and second, it introduces an additional stochastic noise (referred to as *instability noise*) through its fluctuations. While the second contribution can be reduced by increasing the observing time, the first one does not improve with time, like geometric stellar leakage. Geometric and instrumental stellar leakage therefore set a limit on the sensitivity of the nulling interferometer.

- *Sky and instrumental background*—Thermal infrared background emission is produced both by the instrument and its environment, i.e., the Earth atmosphere for ground-based instrument (or the local zodiacal dust cloud for space-based instruments). These contributions are respectively evaluated by night sky brightness measurements (or space-based infrared zodiacal light measurements) and through a detailed modelling of the instrument, taking into account the emissivity and transmission of warm and cold optical elements in the optical path from the telescopes down to the detector.

3.2 Stochastic perturbations and closed-loop control

Stochastic fluctuations of the phase and intensity of the wavefronts that are recombined in the nulling instrument lead to instrumental stellar leakage, which can severely degrade the sensitivity of the instrument. In particular, for ground-based instruments, the Earth atmosphere produces a variety of effects, such as piston, longitudinal dispersion, wavefront corrugations, intensity fluctuations, etc., that must be reduced in order to ensure a deep and stable nulling of the stellar light. Dedicated correction systems are therefore mandatory, and include the following devices:

- *Spatial filtering*—Converts wavefront errors into pure intensity fluctuations by injecting light into a single-more waveguide.
- *Wavefront control*—In order to inject a significant amount of light into the waveguides, low-order adaptive optics (e.g., tip-tilt control) are generally required.
- *Fringe tracking*—A dedicated fringe sensor is used to determine the phase of the two incoming beams and feeds an optical correction system to correct for the piston effect. The correction system usually consists in an optical delay line and/or in a small mirror mounted on a fast piezo motor.
- *Dispersion correction*—Longitudinal dispersion may introduce a significant offset in the beam phases between the wavelength where fringe tracking is done and the wavelength where the destructive output is recorded. Therefore, a dedicated longitudinal dispersion control system may also be required. This device consists in a fringe sensor, working at a different wavelength as the fringe tracking sensor, feeding a dedicated compensation system (e.g., dispersive elements in the optical path, whose thickness can be controlled in real time).
- *Intensity control*—Because single-mode waveguides convert wavefront phase errors into intensity fluctuations, intensity control may be required at the output of the waveguides to ensure a good balance of the two beam intensities. A simple photometer can be used to evaluate the intensities and feed an active compensator (e.g., a tunable iris in each arm of the interferometer).

Control loops are simulated in the frequency domain in GENIEsim: the input perturbations are described by their Power Spectral Densities (PSD), and the effect of real-time servo control simulated by the transfer function of the control loop. The control loop parameters are computed through a simultaneous optimisation of the repetition frequency and of the controller parameters, assuming a simple PID controller. Random time series for the various atmospheric and instrumental stochastic parameters are then generated from the simulated PSDs at the output of the servo loops.

3.3 Post-processing of nulling data

The output of the simulator basically consists in time series of photo-electrons recorded by the detector at the two outputs of the nulling beam combiner (constructive and destructive outputs). Post-processing is an important step towards the detection of faint circumstellar features in nulling interferometry, in order to further disentangle the various contributions to the detected signal. Three main calibration levels are applied to the collected signal:

- *Background subtraction*—We assume that the background is measured simultaneously to the scientific observations, by using off-axis fibres in the field-of-view of the telescopes. In this way, most of the background fluctuations are cancelled out. We assume that the spatial uniformity of the background is such that photon noise is the dominant source of error in background subtraction.
- *Geometric leakage calibration*—Geometric stellar leakage is generally the dominant source of photons at the destructive output of the interferometer. Fortunately, it can be calibrated analytically thanks to Eq. 3 if the stellar angular diameter is known. In the following study, we assume that surface-brightness relationships[7] are used to derive limb-darkened angular diameters of main sequence stars with a typical accuracy of 1%. In that case, the geometric stellar leakage can be removed with an accuracy of 2%.
- *Instrumental leakage calibration*—After these two levels of calibration, the mean instrumental stellar leakage may become the dominant source of noise (or more precisely, of bias). This contribution can be partly calibrated by observing a calibrator star with similar magnitude and colours, so that the control loop performance is equivalent to that obtained on the target star. The calibration measurement is of course affected by its own noise (shot noise, detector noise, instability noise, etc).

The final performance of a nulling interferometer will be expressed in the following study as the lowest density level of an exozodiacal cloud that can be detected at the 5σ level. Smaller numbers will therefore denote higher sensitivities.

Table 1. Atmospheric parameters adopted for the performance simulations of GENIE at Cerro Paranal and ALADDIN at Dome C. In the case of Dome C, the instrument is assumed to be located 30 m above the ground level. The equivalent wind speed is the wind speed integrated across the whole turbulence profile.

Atmospheric parameters	Paranal	Dome C
Fried parameter r_0 at 500 nm	13 cm	38 cm
Equivalent seeing	$0\farcs8$	$0\farcs27$
Coherence time τ_0	3.6 msec	7.9 msec
Equivalent wind speed	11 m/s	15 m/s
Sky/ambient temperature	285 K	230 K
Mean precipitable water vapour	3 mm	0.25 mm
RMS precipitable water vapour	27 μm	1 μm

4. SIMULATED PERFORMANCE FROM THE GROUND

In this section, we evaluate the performance of two proposed ground-based nulling interferometers, which have previously been studied to the pre-phase A or phase A level. The first one was foreseen to be installed on a "classical" astronomical site (Cerro Paranal, Chili), while the second one is considered for an installation at Dome C on the high Antarctic plateau. These two nulling instruments have very similar architectures and work at similar wavelengths (the atmospheric L band), so that a performance comparison between them is meaningful. For performance comparison, we have chosen four hypothetic stars, which are representative of the DARWIN/TPF target catalogue: a K0 V star at 5 pc, a G5 V star at 10 pc, a G0 V star at 20 pc and a G0 V star at 30 pc.

4.1 Performance at a temperate site: GENIE at Cerro Paranal

The Ground-based European Nulling Interferometry Experiment (GENIE) was proposed by the European Space Agency as a technological and scientific precursor to the DARWIN mission, and was considered to be installed at the interferometric focus of the European Southern Observatory's Very Large Telescope Interferometer (VLTI, Cerro Paranal) as part of an ESA/ESO agreement. The instrument, which could operate on either two 8-m Unit Telescopes or two 1.8-m Auxiliary Telescopes, was studied at the Phase A level by two industrial and academic consortia before ESA and ESO decided not to pursue its development.

During the Phase A studies, the expected performance of the GENIE instrument was carefully evaluated with the GENIEsim software,[10] using the typical atmospheric parameters for Cerro Paranal listed in Table 1. The design of GENIE, which is described in a previous paper,[14] basically consists in the following sub-systems. Wavefront control and a first level of piston correction is provided by the VLTI infrastructure (using MACAO/STRAP and PRIMA-FSU). Implemented in the GENIE instrument are fine and fast piston control, longitudinal dispersion correction (which also produces the π phase shift in one arm of the interferometer) and intensity control (see Sect. 3.2). The residuals atmospheric errors after closed-loop control are given in Table 2. After passing through all these sub-systems, the two beams are recombined on a Modified Mach Zehnder[16] (MMZ) beam combiner and injected into single-mode optical fibres before being detected on a standard near-infrared detector.

The simulated performance of the GENIE instrument are displayed on the left-hand side of Fig. 3 as a function of baseline length for the 8-m UTs. Due to the particular arrangement of the VLTI platform, only baselines longer than 46 m are actually available. Such baselines are clearly not optimal for exozodiacal disc detection, so that the sensitivity ranges between 50 zodis in the best case (G0 V star at 20 pc) and a few hundreds zodis in the worst case (K0 V at 5 pc). Observing with the 1.8-m ATs could partially solve this problem, as baselines as short at 8 m would then be available. However, their smaller collecting area does not provide a good sensitivity within reasonable integration times, except for the brightest stars (in particular the K0 V star at 5 pc, for which a sensitivity of about 125 zodis can be reached on the ATs).

4.2 Performance on the high Antarctic plateau: ALADDIN at Dome C

The performance of the GENIE instrument is mostly limited by the inappropriate baseline range provided by the VLTI for the UTs, and by the limited sensitivity of the ATs due to the high thermal background emission in the L band. Residual instability noise after closed-loop correction of atmospheric turbulence is another dominant

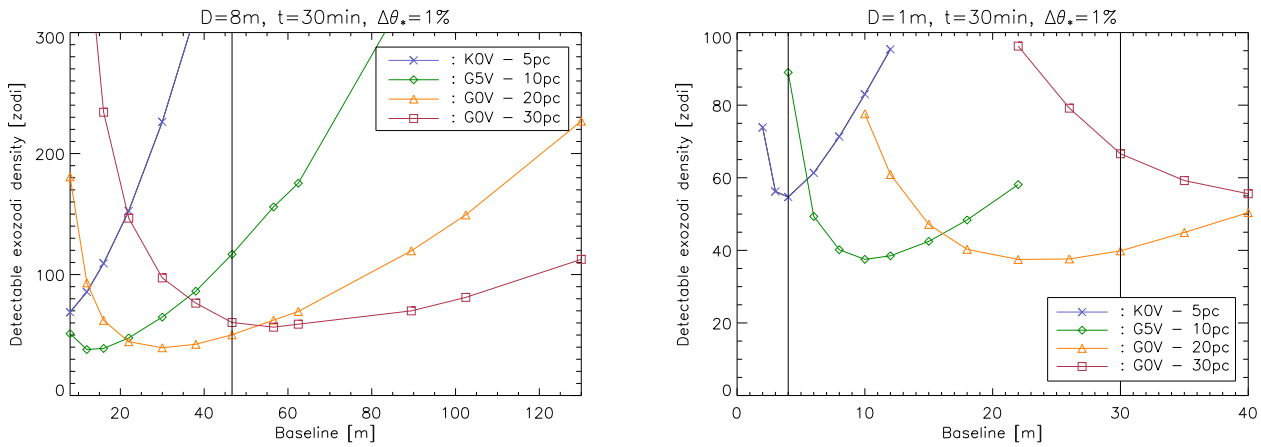

Figure 3. Simulated performance of ground-based nulling interferometers in terms of exozodiacal disc detection for four typical Darwin/TPF targets. *Left*: GENIE at Cerro Paranal using 8-m UTs, for which baselines shorter than 46 m are not accessible. *Right*: ALADDIN at Dome C, for which available baselines range between 4 and 30 m.

contributor in the noise budget. Placing the instrument on the high Antarctic plateau, where the atmosphere is cooler and calmer, using a dedicated infrastructure, is therefore a sensible way to improve its sensitivity. This is the goal of the Antarctic *L*-band Astrophysics Discovery Demonstrator for Interferometric Nulling (ALADDIN), a conceptual copy of the GENIE instrument for which a full instrumental concept has recently been proposed.[15] The infrastructure consists in a 40-m long rotating truss installed on top of a 30 m tower to reduce the effect of the turbulent ground layer, and on which are placed two moveable siderostats feeding 1-m sized off-axis telescopes. Such a design has two main advantages: first, thanks to the moveable siderostats, the baseline length can be optimised to the observed target and second, thanks to the rotating truss, the baseline can always be chosen perpendicular to the line of sight so that neither long delay lines nor dispersion correctors are needed. Moreover, polarisation issues, which are especially harmful in nulling interferometry,[16] are mitigated by this fully symmetric design. The available baseline lengths range from 4 to 30 m and provide a maximum angular resolution of 10 mas.

The nulling instrument works in the *L* band (2.8 to 4.1 μm at Dome C) and follows the original GENIE design adapted to the particular Antarctic conditions. Thanks to the low atmospheric turbulence and water vapour content, the longitudinal dispersion and intensity control loops are not needed any more (this is indicated by a 0 Hz repetition frequency in Table 2), while the piston control loop can be operated at a significantly lower frequency than in the case of GENIE. The whole nulling instrument is assumed to be enclosed in a cryostat, in order to improve its overall stability and to mitigate the influence of temperature variations between seasons at the ground level. Tip-tilt control is implemented inside the instrument to ensure a stable injection into the single-mode optical fibres.

The performance of ALADDIN have been evaluated with GENIEsim, using the atmospheric parameters listed in Table 1. They are summarised as a function of baseline length in Fig. 3. Thanks to the optimised baseline range, as well as to the reduced thermal background and atmospheric turbulence, the sensitivity is improved with respect to that of GENIE on 8-m sized telescopes, and reaches 37 zodis in the best cases (G5 V at 10 pc and G0 V at 20 pc). This sensitivity makes ALADDIN a suitable instrument to screen the Darwin/TPF targets in search for high exozodiacal dust density levels that would prevent from detecting Earth-like planets in the habitable zone. It must also be noted that the sensitivity of ALADDIN to systematic error on the estimated stellar angular diameters can be partly mitigated by performing observations at various baselines and by fitting to the data the stellar angular diameter together with the exozodiacal dust density.[15] Using larger telescopes would not significantly improve the overall sensitivity, which is mostly limited by geometric stellar leakage even for these short baseline lengths.

Table 2. Control loop performance and optimum repetition frequencies computed for a 100 sec observation sequence over the whole wavelength range for each instrument. The observations are carried out for a Sun-like star located at 20 pc using either the 47-m UT2-UT3 baseline at the VLTI (3.5-4.1 μm), a baseline length of 20 m for ALADDIN (3.1-4.1 μm), a 40-m baseline length for PEGASE (1.5-6 μm) and the 12.5-m baseline for FKSI (3-8 μm). The total null is the mean nulling ratio including both the geometric and instrumental leakage contributions. The rms null is the standard deviation of the instrumental nulling ratio. The goal performance for exozodiacal disc detection appears in the last column.

	GENIE-UT	ALADDIN	PEGASE	FKSI	Goal
Piston	6.2 nm @ 13 kHz	10 nm @ 2 kHz	1.7 nm @ 60 Hz	2 nm @ 65 Hz	$<$ 4nm
Inter-band disp.	4.4 nm @ 300 Hz	7.0 nm @ 0 kHz	0 nm @ 0 kHz	0 nm @ 0 kHz	$<$ 4nm
Intra-band disp.	1.0 nm @ 300 Hz	7.4 nm @ 0 Hz	0 nm @ 0 kHz	0 nm @ 0 kHz	$<$ 4nm
Tip-tilt	11 mas @ 1 kHz	7 mas @ 1 kHz	15 mas @ 85 Hz	20 mas @ 60 Hz	(see intensity)
Intensity mismatch	4% @ 1 kHz	1.2% @ 0 Hz	0.02% @ 0 kHz	0.04% @ 0 Hz	$<$ 1%
Total null	6.2×10^{-4}	2.2×10^{-4}	1.0×10^{-3}	3.0×10^{-5}	$f(B, \lambda)$
Instrumental null	1.5×10^{-4}	1.3×10^{-4}	1.0×10^{-5}	7.0×10^{-6}	10^{-5}
RMS null	2.0×10^{-6}	3.5×10^{-6}	1.1×10^{-7}	6.9×10^{-8}	10^{-5}

Table 3. Instrumental parameters of PEGASE and FKSI considered in this study.

Instrumental parameters	PEGASE	FKSI
Baselines [m]	40–500	12.5
Telescope diameter [m]	0.40	0.50
Optics temperature [K]	90 $\pm$ 0.1	65 $\pm$ 0.1
Detector temperature [K]	55 $\pm$ 0.1	35 $\pm$ 0.1
Science waveband [μm]	1.5–6	3–8
Spectral resolution	60	20

5. SIMULATED PERFORMANCE IN SPACE

Further reduction of the thermal infrared background and the turbulence level can be achieved by using space-based instruments. Two space-based interferometric precursors to DARWIN/TPF have recently been proposed: PEGASE and the Fourier-Kelvin Stellar Interferometer (FKSI). They present similar architectures, the main difference being that the two telescopes of PEGASE are free-flying while those of FKSI are arranged on a single boom. PEGASE was initially proposed in the framework of the 2004 call for ideas by the French space agency (CNES) for its formation flying demonstrator mission. CNES performed a Phase 0 study in 2005 and concluded that the mission is feasible within an 8 to 9 years development plan.[17] However, the mission was not selected for budgetary reasons. On the US side, FKSI has been initially studied by the Goddard Space Flight Center in preparation for submission as a Discovery-class mission.[18] Several concepts have been considered and the mission was studied to the phase A level based on the two-telescope design described here.

- PEGASE—The baseline configuration of PEGASE consists in a two-aperture interferometer formed of three free flying spacecraft placed at the Lagrange point L2. Thanks to this location, the spacecraft and the focal plane assembly can be passively cooled down to respectively 90 ± 0.1 K and 55 ± 0.1 K. In its nominal configuration, PEGASE consists in two 40-cm siderostats and a beam combiner flying in linear formation. The interferometric baseline length ranges between 40 m and 500 m giving an angular resolution in the range of 0.5–30 mas for the considered wavelength range (1.5–6 μm). Shorter baseline lengths are not allowed due to the free-flying collision avoidance distance of 20 m.
- FKSI—Resulting from several dedicated studies in the past few years, the FKSI design nowadays consists in two 50-cm telescopes standing at both ends of a 12.5-m boom, giving an angular resolution between 50 and 130 mas for the considered wavelength range (3–8 μm). The instrument is foreseen to be launched to L2 where it will be passively cooled down to 65 K. The field-of-regard is somewhat smaller that the one of PEGASE with possible angles of $\pm 20^\circ$ around the anti-solar direction (vs. $\pm 30^\circ$ for PEGASE). This value depends on the size of the sunshields considered in the present design and could eventually be increased.

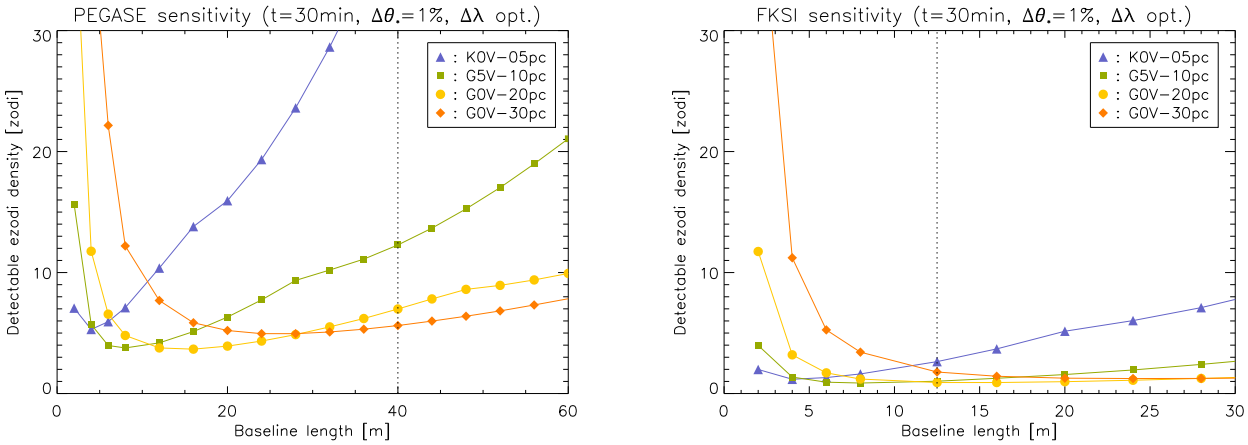

Figure 4. Same as Fig. 3 in the cases of PEGASE (left) and FKSI (right).

The optical path and architecture of PEGASE and the FKSI follow the same general design. The achromatic π phase-shift is achieved geometrically, by means of opposite periscopes producing field reversal by reflections. The fine-tuning of the optical path difference (OPD) is performed by a dedicated control loop based on a fringe sensing unit using the near-infrared part of the signal from the observed central target and a fast optical delay line. Intensity control is performed by a fine pointing loop using a field relative angle sensor and fast steering mirrors based on piezoelectric devices. An MMZ is used to perform beam combination. A second MMZ might be necessary to cover the full wavelength range, depending on the coatings. Small off-axis parabolas are then used to focus the four outputs of the MMZ into single mode fibres, leading the photons directly to the detector. The main instrumental parameters of PEGASE and FKSI are summarised in Table 3.

In order to assess the performance of PEGASE and FKSI for exozodiacal disc detection, GENIEsim was adapted to a space-based environment.[19] Beside disabling all atmospheric effects, the main modification was to introduce the random sequences of OPD and tip/tilt generated by the vibrations of the telescopes in the ambient space environment. These vibrations are related to disturbance forces which can be either internal (caused by on-board systems such as the delay line, the steering mirrors, the reaction wheels, etc.) or external (caused by particulate impacts, solar radiation pressure and charging effects). The PSDs for OPD and tip/tilt disturbances computed by Astrium and CNES[20] during the R&D study of PEGASE have been implemented in GENIEsim.[19] The resonant modes of the boom have been added to the FKSI simulations. The performance of the PEGASE and FKSI control loops is given in Table 2, showing very low instrumental stellar leakage thanks to the reduced phase and intensity perturbations in space. Another difference with ground-based simulations comes from the much wider wavebands of the space-based instruments. Because the various noises have different spectral behaviours, we have implemented a dedicated routine which optimises the chosen wavelength range to maximise the sensitivity to exozodiacal clouds. In practice, the long-wavelength part of the offered wavelength range always provides the best signal-to-noise ratio, but the width of the optimum waveband changes depending on the observation parameters (target, baseline, integration time, etc.).

The expected performance of PEGASE and FKSI are illustrated in Fig. 4 for the four fiducial DARWIN/TPF targets, using an optimised wavelength band for each individual simulation. As in the case of VLTI/GENIE, one can note that the baseline lengths available to PEGASE (> 40 m) are not suited to optimise the sensitivity to exozodiacal clouds, which thus ranges only between 5 and 40 zodis. Conversely, the 12.5-m long FSKI baseline, combined with an appropriate observing wavelength, allows very high sensitivities to be reached (about 1 zodi on all targets). It must be noted that, even with an optimised baseline range, PEGASE would not reach the FKSI sensitivity. This is mainly due to the longer wavelengths offered by FSKI (up to 8 μm), which provide a lower disc/star flux ratio.

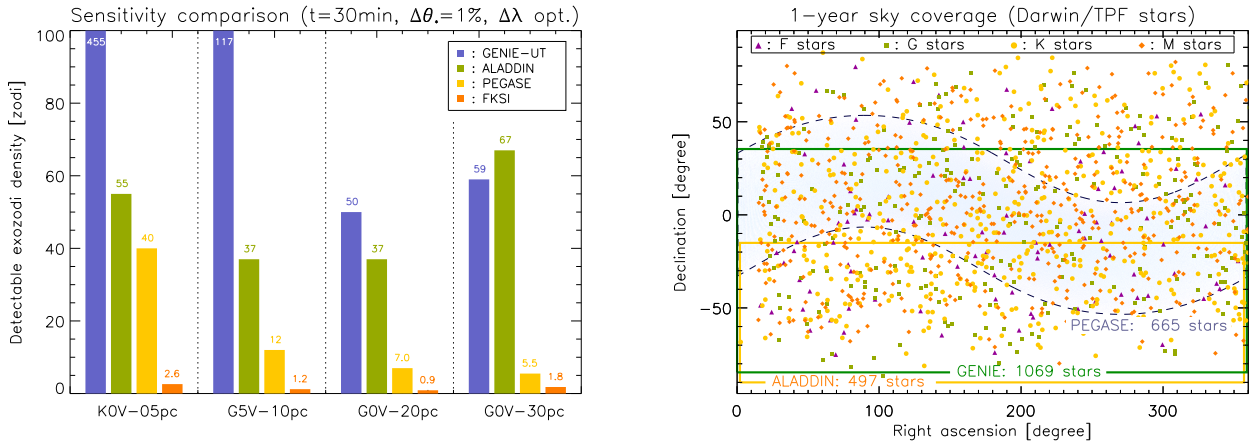

Figure 5. *Left*: Comparison of sensitivities for the four ground-based and spaced-based nulling interferometers considered in this study, for 30 min integration time and 1% uncertainty on the stellar angular diameters. *Right*: Associated sky coverage after one year of observations. The blue-shaded area shows the accessible sky region for a space-based instrument with an ecliptic latitude coverage in the [−30°,30°] range, such as PEGASE.

6. TOWARDS AN OPTIMISED STRATEGY

The detectable exozodiacal densities for GENIE on UTs, ALADDIN, PEGASE and FKSI are compared in Fig. 5, considering an integration time of 30 min and an uncertainty on the stellar angular diameters of 1%. For all target stars, the space-based nulling interferometers are the most sensitive instruments. PEGASE (resp. FKSI) outperforms ALADDIN by a factor ranging from about 1.5 (resp. 20) for the K0 V star located at 5 pc to a factor of about 10 (resp. 30) for the G0 V star located at 30 pc. This better sensitivity of space-based instruments is mainly due to the lower thermal background and geometric stellar leakage, which are both dominant noises for GENIE and ALADDIN. While the absence of atmosphere in space and cooler optics explain the lower thermal background, the longer observing wavelength has the advantage to improve the geometric stellar rejection which is proportional to the squared wavelength. The access to the DARWIN/TPF targets as a function of position in the sky is represented for three instruments on the right-hand side of Fig. 5. The sky coverage for FKSI is similar to that of PEGASE, although with a reduced width.

The conclusion of this study is that a structurally-connected space-based interferometer working in the mid-infrared (6–8 μm) such as FKSI is the most suited nulling instrument for obtaining resolved detections of faint exozodiacal dust clouds around nearby main sequence stars. It allows exozodiacal discs as faint a our local zodiacal cloud to be detected and characterised with low-resolution spectroscopy and aperture synthesis. Such an instrument would additionally provide a wealth of valuable scientific information on the formation and evolution of dusty discs around main sequence stars, including dust production processes and dynamical interactions with larger bodies. However, if a "cheap" way is required to prepare the DARWIN/TPF science programme by identifying target stars surrounded by too large an amount of dust ($>$ 20 zodis), a nulling interferometer in Antarctica such as ALADDIN would probably be a very wise first step: with typical integration times of about 4 hours per target, it would allow sensitivities in the range 20–40 zodis for most of the Southern targets. This mission could be achieved within one single winter-over at Dome C. Such a mission would also provide valuable statistical constraints on the correlation between the amount of exozodiacal dust and various stellar parameters, that could then be used to refine the target choice across the whole sky.

REFERENCES

[1] Grün, E., Gustafson, B. A. S., Dermott, S., and Fechtig, H., eds., [*Interplanetary dust*], Berlin: Springer (2001).

[2] Gurnett, D. A., Ansher, J. A., Kurth, W. S., and Granroth, L. J., "Micron-sized dust particles detected in the outer solar system by the Voyager 1 and 2 plasma wave instruments," *Geophys. Res. Lett.* **24**, 3125–3128 (1997).

[3] Beichman, C. A., Bryden, G., Stapelfeldt, K. R., et al., "New Debris Disks around Nearby Main-Sequence Stars: Impact on the Direct Detection of Planets," *ApJ* **652**, 1674–1693 (2006).

[4] Bryden, G., Beichman, C. A., Trilling, D. E., et al., "Frequency of Debris Disks around Solar-Type Stars: First Results from a Spitzer MIPS Survey," *ApJ* **636**, 1098–1113 (2006).

[5] Di Folco, E., Absil, O., Augereau, J.-C., et al., "A near-infrared interferometric survey of debris-disk stars. I. Probing the hot dust content around ϵ Eri and τ Cet with CHARA/FLUOR," *A&A* **475**, 243–250 (2007).

[6] Kervella, P., Thévenin, F., Ségransan, D., et al., "The diameters of alpha Centauri A and B. A comparison of the asteroseismic and VINCI/VLTI views," *A&A* **404**, 1087–1097 (2003).

[7] Kervella, P., Thévenin, F., di Folco, E., and Ségransan, D., "The angular sizes of dwarf stars and subgiants: Surface brightness relations calibrated by interferometry," *A&A* **426**, 297–307 (2004).

[8] Serabyn, E., "First deep nulling science observations with the Keck interferometer nuller," in [*Optical and Infrared Interferometry*], Schöller, M., Danchi, W. C., and Delplancke, F., eds., *Proc. SPIE* **7013** (2008).

[9] Di Folco, E., Thévenin, F., Kervella, P., et al., "VLTI near-IR interferometric observations of Vega-like stars," *A&A* **426**, 601–617 (2004).

[10] Absil, O., Di Folco, E., Mérand, A., et al., "Circumstellar material in the Vega inner system revealed by CHARA/FLUOR," *A&A* **452**, 237–244 (2006).

[11] Absil, O., Di Folco, E., Mérand, A., et al., "A near-infrared interferometric survey of debris-disk stars. II. CHARA/FLUOR observations of six early-type dwarfs," *A&A* (2008), submitted.

[12] Absil, O., den Hartog, R., Gondoin, P., et al., "Performance study of ground-based infrared Bracewell interferometers – Application to the detection of exozodiacal dust disks with GENIE," *A&A* **448**, 787–800 (2006).

[13] Kelsall, T., Weiland, J. L., Franz, B. A., et al., "The COBE Diffuse Infrared Background Experiment Search for the Cosmic Infrared Background. II. Model of the Interplanetary Dust Cloud," *ApJ* **508**, 44–73 (1998).

[14] Gondoin, P. A., Absil, O., den Hartog, R. H., et al., "Darwin-GENIE: a nulling instrument at the VLTI," in [*New Frontiers in Stellar Interferometry*], Traub, W., ed., *Proc. SPIE* **5491**, 775–786 (2004).

[15] Absil, O., Coudé du Foresto, V., Barillot, M., and Swain, M. R., "Nulling interferometry: performance comparison between Antarctica and other ground-based sites," *A&A* **475**, 1185–1194 (2007).

[16] Serabyn, E. and Colavita, M. M., "Fully Symmetric Nulling Beam Combiners," *Appl. Opt.* **40**, 1668–1671 (2001).

[17] Le Duigou, J. M., Ollivier, M., Léger, A., et al., "Pegase: a space-based nulling interferometer," in [*Space Telescopes and Instrumentation I: Optical, Infrared, and Millimeter*], Mather, J. C., MacEwen, H. A., and de Graauw, M., eds., *Proc. SPIE* **6265**, 6265–1M (2006).

[18] Danchi, W. C., Barry, R. K., Deming, D., et al., "Scientific rationale for exoplanet characterization from 3-8 microns: the FKSI mission," in [*Advances in Stellar Interferometry*], Monnier, J. D., Schöller, M., and Danchi, W. C., eds., *Proc. SPIE* **6268**, 6268–20 (2006).

[19] Defrère, D., Absil, O., Coudé du Foresto, V., et al., "Nulling interferometry: performance comparison between space and ground-based sites for exozodiacal disc detection," *A&A* (2008), submitted.

[20] Villien, A., Morand, J., Delpech, M., and Guidotti, P.-Y., "GNC for the Pegase Mission," *17th IFAC Symposium on Automatic Control in Aerospace* (2007).